JOURNAL OF Materials CHEMISTRY

TOF-SIMS characterization of the surface of monophase hybrid organic inorganic materials

Geneviève Cerveau,[a] Robert J. P. Corriu,*[a] Josiane Dabosi,[a] Jean-Louis Aubagnac,[b] Robert Combarieu[c] and Yves de Puydt[c]

[a]*Laboratoire de Chimie Moléculaire et Organisation du Solide, UMR 5637, Université Montpellier II, Case Courrier 007–34095 Montpellier Cedex 5, France*

[b]*UMR 5810, Laboratoire des Aminoacides, Peptides et Protéines, Université Montpellier II, 34095 Montpellier Cedex 5, France*

[c]*UMR 7635 CEMEF, Ecole des Mines de Paris, 06904 Sophia Antipolis Cedex, France*

TOF-SIMS (time of flight secondary ion mass spectrometry) has been used to analyse the surface composition of monophasic hybrid organic–inorganic materials (MHOIM). Gels of type $RSiO_{1.5}$ obtained from monosilylated precursors $RSi(OR')_3$, (with R′ = Me, Et and R = hydrogen, alkyl, halogenoalkyl, alkenyl, aromatic and ferrocenyl units) have been analysed and in each case, characteristic mass fragment ions of R groups have been detected and clearly identified owing to the high mass resolution of TOF-SIMS. The large variety of precursors used allows one to conclude that the monosilylated precursors lead, as expected, to solids in which the organic moiety is located at the surface. Thus TOF-SIMS appears to be an efficient tool for the detection of groups located at the surface of amorphous hybrid systems.

Introduction

Sol–gel processes have recently proved to be of great interest for the elaboration of hybrid organic–inorganic mono- or poly-phasic materials.[1] We are interested in the preparation and characterization of monophasic hybrid materials obtained by hydrolysis and polycondensation of substituted trialkoxysilanes containing non-hydrolysable Si—C bonds.[2] The resulting polyorganosils esquioxanes are three-dimensional network materials in which the organic fragment is an integral component of the network and is covalently bound to silica (Scheme 1). Their chemical composition has been determined by a number of spectroscopic techniques including solid-state ^{13}C and ^{29}Si CP MAS NMR which show that the Si—C bond is completely maintained during the solid formation. However it is important to determine the location of the organic moieties which can be either at the surface or in the bulk of the solid. In previous work we have shown that the electrochemical behaviour or the chemical reactivity of hybrid silica are reliable tools for determining the location of the organic entities. For example: (i) gels formed from 1,1′-bis(trimethoxysilyl)ferrocene display a cottrellian diffusion of charge transfer in accordance with most of the ferrocene moieties being located in the bulk of the solid, while in the case of gels obtained from trimethoxysilylferrocene, the charge transfer follows a power law with a fractional exponent, indicative of the accessibility of ferrocene moieties at the surface of silica particles.[3]

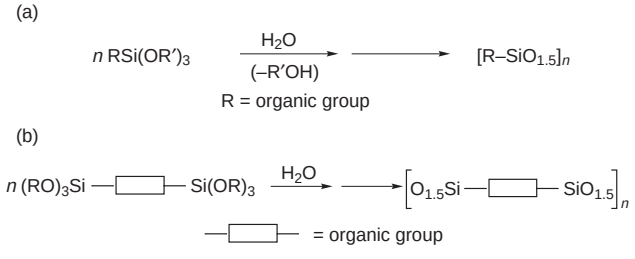

Scheme 1 Hydrolysis–polycondensation of organotrialkoxysilanes

(ii) The reactivity of phenyl groups attached to a silica network, towards complexation with $Cr(CO)_6$ has been used to test the accessibility of aromatic groups in silica matrices. In the case of gels obtained from monosilylated phenyl compounds, the introduction of $Cr(CO)_6$ is possible since most of the phenyl groups are located at the surface of silica,[4] while for bis-silylated phenylene compounds the chemical behaviour is highly dependent on the nature, rigid or flexible, of the precursor. When the precursor contains rigid phenylene units, the resulting solid is hydrophilic and the organic units, located in the core of the solid are poorly accessible for chemical reactions. In contrast, when more flexible organic groups such as phenylene-1,4-bis(ethylene) are introduced, the solid is hydrophobic and reacts with $Cr(CO)_6$, since the phenylene groups are present at the surface.[5]

(iii) In functional gels formed from $HSi(OEt)_3$ and containing Si—H bonds, the high reactivity of the Si—H has been demonstrated. Molecular oxygen and ammonia react with formation of silica and oxynitride materials, respectively.[6,7]

Specific tailored organic surfaces are becoming increasingly important for various applications in order to optimize the surface properties influencing, *e.g.* wetting behaviour, adhesion, long term stability, and biocompatibility. Sol–gel processes can offer the possibility of variable molecular architecture, so an efficient surface characterization is required. Such surface information should be supplied with high sensitivity not only for the elemental but also for the molecular composition.

Up to now, spectroscopic methods such as NMR and IR have been used to characterise these compounds but no information about surface properties can be obtained. Time-of-flight (TOF) SIMS is now widely used for polymer surface characterization.[8–10] For bulk polymers, the fingerprint spectrum ($m/z < 200$) contains fragments specific to the molecular structure of the polymers and allows identification of most of them. Static SIMS supplies molecular informations on the surface, particularly on the specific tailored organic radicals. The higher mass resolution obtained in TOF-SIMS spectra is useful to define further the identity of fragment ions. Higher sensitivity owing to the overall transmission efficiency of the mass analysor, can be obtained with TOF-SIMS compared with quadrupole static SIMS.

We report here a systematic investigation of secondary ion formation from hybrid materials containing only one Si—C bond of type $RSiO_{1.5}$ obtained by hydrolysis–polycondensation of monosilylated precursors (Scheme 2).

Experimental

Solvents were dried and distilled before use. Melting points were determined with a Gallenkamp apparatus and are uncorrected. ^{1}H NMR spectra were recorded on a Bruker DPX 200 spectrometer, ^{13}C and ^{29}Si NMR spectra in solution on a Bruker AC 250 and solid state cross polarization magic angle spinning (CP MAS) ^{29}Si and ^{13}C spectra with a Bruker FT-AM 300 spectrometer. Solvents and chemical shifts (δ relative to Me_4Si) are indicated. The specific surface areas were determined by analysing N_2 adsorption–desorption isotherms according to the BET method using a Micromeritics Gemini 2360 apparatus. Combustion analyses were carried out by the Service Central de Micro-Analyse du CNRS. TOF-SIMS investigations were performed on a TRIFT I spectrometer (Charles Evans & Associates).

Starting monomers

The starting monomers chloromethyltrimethoxysilane **3**, 3-iodopropyltrimethoxysilane **5**, 3-aminopropyltrimethoxysilane **6**, (2-phenethyl)trimethoxysilane **12**, *N*-phenylaminopropyltrimethoxysilane **13**, and 2-(diphenylphosphino)ethyltriethoxysilane **14** were purchased from Gelest. [2-(Dimethylaminomethyl)phenyl]trimethoxysilane **9** and [8-(dimethylamino)-1-naphthyl]trimethoxysilane **11** were prepared according to literature procedures.[11]

Preparation of 1-(*N*,*N*′-dimethylaminomethyl)-2-(trimethoxysilyl)ferrocene 16. 1-(*N*,*N*′-dimethylaminomethyl)-2-lithioferrocene prepared according to ref. 12 from 12.15 g (50 mmol) of (*N*,*N*′-dimethylaminomethyl)ferrocene and 25 ml (62.5 mmol, 2.5 M in hexane) of Bu^{n}Li was added dropwise to 9.5 g (60 mmol) of $ClSi(OMe)_3$ in 50 ml diethyl ether at room temperature. A precipitate formed immediately and the reaction mixture was stirred for 3 h. The mixture was then filtered and the salts washed with diethyl ether. The solvent was evaporated *in vacuo* and the residue distilled. A 14.33 g amount (79%) of trimethoxy precursor was recovered; bp 126–129 °C (≈1.3 Pa). ^{1}H NMR ($CDCl_3$) δ 2.16 (6H, s, NCH_3), 3.22 and 3.42 (2 × 1H, 2d, diastereotopic protons CH_2N), 3.66 (9H, s, OCH_3), 4.15 (5H, s, C_5H_5), 4.36 (3H, br, C_5H_3). ^{13}C NMR ($CDCl_3$) δ 45.2 (NCH_3), 51.1 (OCH_3), 59.1 (CH_2N), 69.5, 71.2, 73.9, 75, 90 (C_5H_3), 69.7 (C_5H_5). ^{29}Si NMR ($CDCl_3$) δ −47.27. Elemental analysis. Found: C, 53.01; H, 6.83; N, 3.58; Fe, 15.31; Si, 7.70. Calc. for $C_{16}H_{25}FeNO_3Si$: C, 52.88; H, 6.95; N, 3.86; Fe, 15.37; Si, 7.73%.

Hydrolysis–polycondensation of trialkoxysilane precursors

The concentration of the precursors and the catalyst, the specific surface areas, the hydrophilicities $E_{0.6}$ and the ^{29}Si NMR data of the new xerogels are listed in Table 1. In all cases, the solids were obtained in quantitative yield based on the ideal stoichiometry $RSiO_{1.5}$. The preparations of silsesquioxane materials were carried out according to the following general procedure. The hydrolysis of 3-iodopropyltrimethoxysilane **5** is given as an example.

Xerogel X5. To 2.9 g (10 mmol) of 3-iodopropyltrimethoxysilane **5** in 1.45 ml of methanol were added 0.54 ml (30 mmol) of water and the catalyst. The homogeneous solution was allowed to stand at room temperature. A precipitate appeared slowly and the mixture was allowed to stand for 4 days at room temperature. The solid was extracted, ground in a mortar, then washed with acetone and water to remove the catalyst, then washed with diethyl ether and dried at 120 °C *in vacuo* to yield 2.2 g of a white powder **X5** (quantitative yield based on $C_3H_6IO_{1.5}Si$). ^{13}C CP MAS NMR, δ 13.5, 15.5, 28.4. Elemental analysis. Found: C, 15.96; H, 2.83; I, 55.76%, Si, 12.5. Calc. for $C_3H_6IO_{1.5}Si$: C, 16.29; H, 2.71; I, 57.47; Si, 12.67%.

Xerogel 12. No gel could be obtained by direct hydrolysis of phenethyltrimethoxysilane. A co-condensation with $Si(OMe)_4$ was thus performed as follows. To 1.13 g (5 mmol) of (2-phenethyl)trimethoxysilane and 0.76 g (5 mmol) of $Si(OMe)_4$ in 9.66 ml of methanol were added 0.32 ml (17.5 mmol) of water and the catalyst. The solution was allowed to stand at room temperature. A solid formed after 7 days. The treatment was the same as above and yielded a white solid. ^{13}C CP MAS NMR, δ 14.6, 29.0, 128.3, 143.5. Elemental analysis. Found: C, 41.03; H, 4.39; Si, 26.40. Calc. for $C_8H_9O_{3.5}Si_2$: C, 44.23; H, 4.15; Si, 25.81%.

^{13}C NMR data and the elemental analyses of new xerogels are reported in Table 2. The preparation of hydrogenosilsesquioxane **X1**,[6] methylsilsesquioxane **X2**,[13] vinylsilsesquioxane **X4**,[14] phenylsilsesquioxane **X8**,[15] ferrocenylsilsesquioxane **X15**[16] have already been reported.

TOF-SIMS analysis

The primary ions are usually generated by a pulsed (1 ns, 12 kHz) monoisotopic $^{69}Ga^+$ source (15 keV); in some cases, a $^{115}In^+$ source was used. The secondary ions were accelerated to an energy of ±3 keV operating in positive or negative mode. The analysed surface is a square of about 100 × 100 μm^2. The total ion dose for acquisition of a spectrum is about 10^{11} ions cm^{-2} ensuring static conditions to avoid detectable ion damage on the surface. The necessary charge compensation was done by means of a pulsed electron flood gun (20 eV kinetic energy) with a rate of one pulse for five Ga^+ pulses.

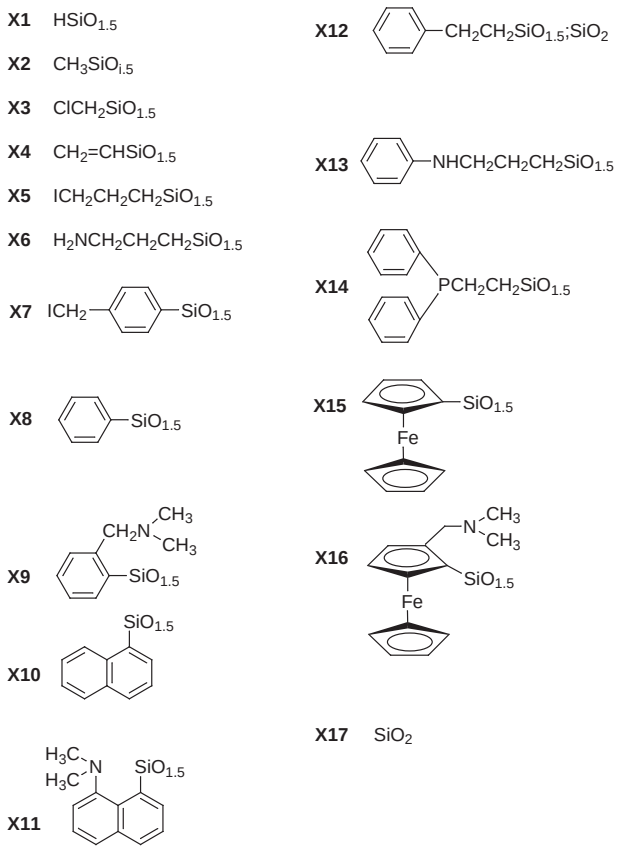

Scheme 2 Xerogels **X1**–**X17**

Table 1 Preparation, specific surface area, hydrophilicity and ^{29}Si CP MAS NMR spectra of new xerogels

xerogel	precursor conc/M	catalyst[a] conc. (mol equiv.)	surface area[b]/ $m^2\ g^{-1}$	$E_{0.6}$[c] (%)	^{29}Si CP MAS NMR[d] (δ)
X3	1	10^{-2}	1.6	1.7	−68.6, **−78.6**
X5	5	3×10^{-2}	1.3	0.14	−58.8, **−67.6**
X6	1	10^{-2}	8.2	5.84	−59.7, **−67.4**
X7	5	3×10^{-2}	1.2	1.25	−70.1, **−78.7**
X9	1	10^{-2}	2.1	0.55	**−80.4**
X10	1	10^{-2}	—	—	−68, **−76.5**
X11	1	10^{-2}	—	—	**−70.9**
X12[e]	1	10^{-2}	0.18	1.67	−59.7, −64.6, −101.1, −109.3
X13	5	3×10^{-2}	—	—	—[f]
X14	5	3×10^{-2}	—	—	−59, **−66.7**
X16	1	10^{-3}	—	—	**−60.8**

[a]Catalyst NH_4F. [b]BET surface area from multipoint analysis of N_2 adsorption isotherm. [c]% weight increase in a 60% humidity atmosphere at 25 °C. [d]Major resonances are in bold. [e]Gel obtained by co-condensation with $Si(OMe)_4$: signals δ at −101.1 and −109.3 correspond to silica. [f]Not determined, waxy solid.

Table 2 ^{13}C NMR spectra and elemental analyses of new xerogels

		elemental analysis							
		calc. (%)[a]				found (%)			
xerogel	^{13}C CP MAS NMR (δ)	C	H	Si	Y[b]	C	H	Si	Y[b]
X3	25	7.45	2.40	28.10	28.66 (Cl)	11.82	1.97	27.59	34.98
X5	13.5, 15.5, 28.4	16.29	2.71	12.67	57.47 (I)	15.96	2.83	12.50	55.76
X6	10, 28, 45.6	32.73	7.27	25.45	12.73 (N)	28.30	7.37	23.90	10.97
X7	19.5, 129.2, 135.1, 142.3	31.23	2.23	10.41	47.21 (I)	32.28	2.36	11.40	43.76
X9	45.2, 64.1, 126.4, 128.6, 131, 136.7, 147[c]	58.07	6.45	15.05	7.53 (N)	57.61	6.53	15.89	7.41
X10	128, 133, 136.3[c]	67.04	3.91	15.64		66.08	4.64	13.60	
X11	49, 118.3, 125.7, 130.3, 134.9, 137.8, 153.3	64.86	5.41	12.61	6.31 (N)	60.20	5.93	10.65	5.46
X12	14.6, 29, 128.3, 143.5	44.23	4.15	25.81		41.03	4.39	26.40	
X13	—[d]	58.07	6.45	15.05	7.53 (N)	57.74	6.56	14.60	7.31
X14	8.7, 20.7, 129, 133, 139.1[c]	63.40	5.28	10.57	11.70 (P)	61.80	5.33	10.75	9.25
X16	43.5, 48.6, 59.7, 66.2, 69.8, 73.9, 87.3	53.06	5.44	9.52	4.76 (N) 19.60 (Fe)	49.59	5.46	9.10	4.60 17.62

[a]Deduced from ideal stoichiometry $RSiO_{1.5}$. [b]Y = element indicated in parentheses. [c]In acetone d_6 solution. [d]Waxy solid not determined.

TOF-SIMS spectra result not only from the ionisation of molecules in the uppermost layers of the surface (about 1 nm), giving molecular ions or fragment ions from $RSiO_{1.5}$, but also from rearrangement products in the plasma formed near the surface.

The high surface sensitivity of this technique indicates the need for pure samples. For this reason, before analysis, all the xerogels were washed in a Soxhlet with refluxing THF for 8 h. However some impurities can still appear on the suface of the powders and ions corresponding to these impurities can be detected. For example, the presence of reagents such as $RSi(OCH_3)_3$ characterised by peaks for $SiOCH_3^+$ at $m/z=59$, $HSi(OCH_3)_2^+$ at $m/z=91$ and $Si(OCH_3)_3^+$ at $m/z=121$ as well as the catalyst NH_4F with $^{19}F^-$ or other very characteristic ions C_xF_y can arise from the sol–gel process. Very often, prominent peaks (m/z 28, 43, 73, 59, 147… marked by an asterisk on the spectra) due to polydimethylsiloxane impurity are observed. In these cases, an additional cleaning of the samples is necessary to eliminate them for a better identification of spectra.

High mass resolution is a great advantage of TOF-SIMS compared with quadrupole static SIMS; mass resolution ($m/\Delta m$) on an Si wafer can reach 10 000, while analyses of powders employed here leads to a lower mass resolution of *ca.* 2000 due to the powder size and to insulating samples. However, these values are generally sufficient for a good mass identification of fragment ions originating from R groups detected on the sample surfaces and to separate, for example, $SiCH_3^+$ from $C_3H_7^+$ at $m/z=43$ [Fig. 1(a)] and implanted primary ions $^{69}Ga^+$ from organic ions [Fig. 1(b)].

The most intense peak in the spectra is always $^{28}Si^+$, which may be due to the fact that atomic ions are less surface sensitive than larger molecular ions.[17] Hydrocarbon C_xH_y peaks which are observed as fragments from the aliphatic chain of the radical R are also prominent. The presence of $SiOH^+$ ions at $m/z=45$ is also very often detected, this peak reflects both real surface SiOH species as well as rearrangment products from silicon, oxygen and hydrogen ions in the plasma at the surface.

Results and discussion

The hydrolysis and polycondensation of precursors **1**–**17** was carried out under nucleophilic catalysis conditions using fluoride ion.[18] In most cases oily and waxy solids formed after various reaction times. After aging for 8 days, they were washed with acetone and diethyl ether, then ground to give powders. Some of the resulting white solids were slightly soluble in acetone and melt. They were analysed by spectroscopic techniques and elemental analyses and data obtained are reported in Table 1. The data are in accord with the conservation of the organic moiety bonded to the silica matrix. The absence of any silica-like resonance in the range δ −100 to −110[19] in the ^{29}Si NMR spectra is consistent with the absence of cleavage of the Si−C bond. Futhermore the ^{13}C NMR spectra of the

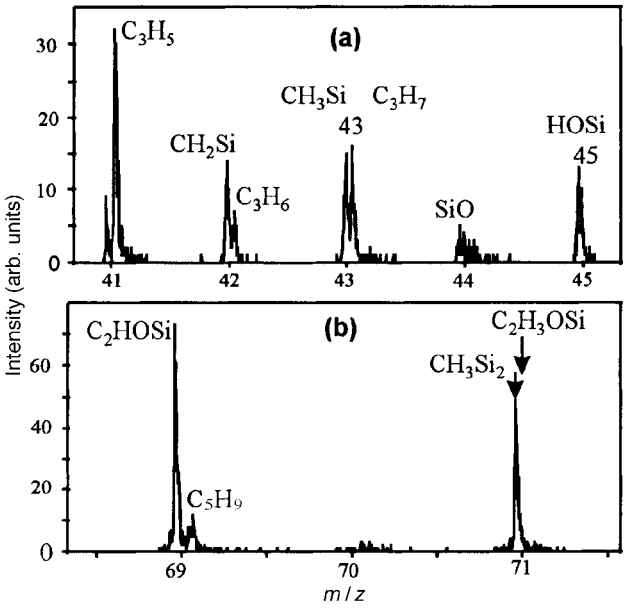

Fig. 1 High mass resolution TOF-SIMS spectrum of $CH_2{=}CHSiO_{1.5}$ **X4**; (a) *m/z* 41–45, (b) *m/z* 69–71

solids are of interest, since they clearly establish that the organic moiety is not affected during the polymerization process (see Experimental section). The solids appear to be highly polycondensed with the T_3 substructure of branched silicates as the major silicon environment.[20] They are generally oligosilsesquioxanes rather than highly crosslinked networks,[21] this is in accord with solids containing organic groups as pendant functionalities of the network polymer.[22] The very low affinity for water of these solids ($E_{0.6}$ as measured by the increase in weight in a 60% humidity atmosphere at 25 °C) indicates that the hydrophobic organic groups are located at the surface. Furthermore the BET surface areas of the hybrid gels **X** are very low in each case.

TOF-SIMS characterisation of the topmost layer

Table 3 summarises the main ions observed in the TOF-SIMS spectra of xerogels **X1**–**X17**.

Table 3 Main ions observed in TOF-SIMS of gels **X1**–**X17** (major fragments are in bold)

xerogel	ions
X1	**29** $(SiH)^+$, **45** $(SiOH)^+$, 73 $(Si_2OH)^+$
X2	**15** $(CH_3)^+$, **43** $(SiCH_3)^+$
X3	**49/51** $(ClCH_2)^+$, 77/79 $(ClCH_2Si)^+$, **35/37** $(Cl)^-$
X4	**14** $(CH_2)^+$, **15** $(CH_3)^+$, **45** $(SiOH)^+$, 55 $(CH_2{=}CHSi)^+$, 69 $(C_2HSiO)^+$
X5	**127** $(I)^+$, **141** $(ICH_2)^+$, **155** $(ICH_2CH_2)^+$, **127** $(I)^-$, 139 $(CI)^-$, **141** $(ICH_2)^-$, **254** $(I_2)^-$, **383** $(I_3)^-$
X6	**18** $(NH_4)^+$, **30** $(CH_2{=}NH_2)^+$, 44 $(H_2NCH_2CH_2)^+$
X7	**127** $(I)^+$, **77** $(C_6H_5)^+$, **141** $(ICH_2)^+$, 217 $(ICH_2C_6H_4)^+$
X8	**77** $(C_6H_5)^+$
X9	**58** $(CH_2{=}NMe_2)^+$, **134** $(C_9H_{12}N)^+$
X10	**127** $(C_{10}H_7)^+$, **155** $(C_{10}H_7Si)^+$
X11	**44** $(C_2H_6N)^+$, **154** $(C_{11}H_8N)^+$, **170** $(C_{12}H_{12}N)^+$
X12	77 $(C_6H_5)^+$, 91 $(C_7H_7)^+$, **105** $(C_8H_9)^+$
X13	**77** $(C_6H_5)^+$, 91 $(C_7H_7)^+$, **106** $(CH_2{=}NHC_6H_5)^+$, **120** $(C_8H_{10}N)^+$, **134** $(C_9H_{12}N)^+$, **92** $(C_6H_5NH)^-$
X14	77 $(C_6H_5)^+$, 91 $(C_7H_7)^+$, **109** $(C_6H_5PH)^+$, **123** $(C_6H_5PCH_3)^+$, **183** $(C_{12}H_8P)^+$, 185 $[(C_6H_5)_2P]^+$
X15	**56** $(Fe)^+$, **65** $(C_5H_5)^+$, **121** $(C_5H_5Fe)^+$, **65** $(C_5H_5)^-$
X16	**56** $(Fe)^+$, **58** $(CH_2{=}NMe_2)^+$, **121** $(C_5H_5Fe)^+$, **134** $(C_6H_6Fe)^+$, **186** $(C_{10}H_{10}Fe)^+$
X17	**28** $(Si)^+$, **45** $(SiOH)^+$

Fig. 2 shows the spectra of silica SiO_2 **X17** and of a first series of xerogels **X1, X2, X4** in which the organic unit R is small and directly bound to silicon (R = H, CH_3, $CH_2{=}CH$). A comparison between the spectra of this series shows that the main characteristic peaks of each organic radical R are always found. For SiO_2, the peak at *m/z* = 45 indicates the presence of OH groups at the surface. High relative intensities of peaks SiH^+ at *m/z* = 29 and Si_2OH^+ at *m/z* = 73, respectively *vs.* $^{28}Si^+$ and Si_2O^+ at *m/z* = 72 appear to be characteristic of gel $HSiO_{1.5}$ **X1**. A significant presence of the peak $SiOH^+$ at *m/z* = 45 shows that Si—O bonds are also accessible owing to the small size of radical R. For gel $CH_3SiO_{1.5}$ **X2**, peaks CH_3^+ at *m/z* = 15 and $SiCH_3^+$ at *m/z* = 43 are characteristic because the peak at *m/z* = 43 cannot originate from impurities such as polydimethylsiloxane due to the lack of other peaks at *m/z* = 73, 147… For $CH_2{=}CHSiO_{1.5}$ **X4**, high mass resolution with TOF-SIMS allowed us to identify C_xH_y from $C_xH_ySi^+$ ions. Positive ion mass spectra show many peaks for each mass unit: at *m/z* = 55, $C_2H_3Si^+$ ion can be distinguished from $C_4H_7^+$ ions [Fig. 1(b)] and the peak at *m/z* = 71 can clearly be identified as $CH_3Si_2^+$ rather than $C_2H_3SiO^+$. Besides the presence of C_xH_y peaks from the vinyl radical, the main characteristic peaks are $C_2H_3Si^+$ at *m/z* = 55 and C_2HSiO^+ at *m/z* = 69.

For xerogels **X3**, **X5**, **X13**, **X14**, containing a functional group linked to silicon through an aliphatic chain, the main ions corresponding to a step-by-step cleavage of the chain are generally observed in the positive mode (Fig. 3).

When an halogen is present, the halogen anion is clearly observed in the negative mode and other characteristic peaks of the group R are identified in the positive mode: for example, for $ClCH_2SiO_{1.5}$ **X3**, the main fragments $ClCH_2^+$ (*m/z* = 49/51), $SiCl^+$(63/65), $ClCH_2Si^+$ (77/79) are present. For $ICH_2CH_2CH_2SiO_{1.5}$ **X5** in positive mode, peaks $^{127}I^+$, ICH_2^+ (141), ISi^+ (155), $I\,C_3H_8^+$ (171) and ICH_2SiO^+ (173) correspond to the step-by-step cleavage of the radical R and in negative mode, peaks $^{127}I^-$, IC^- (139), ICH_2^- (141), IO^- (143), $ICH_2CH_2^-$ (155), $ISiO^-$ (171), $ISiO_2^-$ (187), I_2^- (254), I_3^- (383) are present.

When R contains an amino or a phosphino group, the most abundant peaks correspond to stable immonium[23] or arylphosphonium ions.[24] For example, for $C_6H_5NHCH_2CH_2CH_2SiO_{1.5}$ **X13**, peaks $C_6H_5^+$, $C_7H_7^+$, $CH_2{=}NHC_6H_5^+$ (106), $C_8H_{10}N^+$ (120) and $C_9H_{12}N^+$ (134) are present in positive mode. In negative mode, peak $C_6H_5NH^-$ (92) is observed. For $(C_6H_5)_2PCH_2CH_2SiO_{1.5}$ **X14**, $C_6H_5^+$, $C_7H_7^+$, $C_6H_5PH^+$ (109), $C_6H_5PHCH_2^+$ (123), $C_{12}H_8P^+$ (183) and $(C_6H_5)_2P^+$ (185) are present in positive mode. Negative ion spectra also show numerous peaks from organic radicals such as $C_6H_6P^-$ (109), $C_{12}H_8P^-$ (183), $(C_6H_5)_2P^-$ (185), $(C_6H_5)_2PCH_2^-$ (199) and $(C_6H_5)_2PCH_2CH_2^-$ (213).

For gels containing a substituted aromatic group directly linked to silicon **X7** and **X9**, characteristic peaks from ICH_2 or $CH_2N(CH_3)_2$ are observed, respectively. In negative mode, halogen anions are always readily observed but in positive mode, higher mass ions are also identified such as ICH_2^+ (141) and $ICH_2C_6H_4^+$ (217) for **X7**. For **X9**, the stable immonium ion $C_3H_6N^+$at *m/z* = 58 and ions from higher mass fragments $(CH_3)_2NCH_2C_6H_4^+$(134) and $(CH_3)_2NCH_2C_6H_4SiO^+$ (178) are observed. By contrast, peaks from unsubstituted aromatic chains such as $C_6H_5^+$ or tropylium ion ($C_7H_7^+$) are at best weak, which may be due to the weak ionization yield of the aromatic ring (*e.g.* **X8**).

For $C_{10}H_7SiO_{1.5}$ gel **X10** (Fig. 4), a characteristic ion $C_{10}H_7^+$ at *m/z* = 127 from the naphthalenic ring is observed. Other peaks such as $C_{10}H_7Si^+$ (155) and $C_{10}H_7OSi^+$ (171) indicating possible ionization of higher mass fragments of the molecule are also identified. For gel **X11**, naphthalenic peaks, immonium group $(CH_3)_2N^+$ at *m/z* = 44 and other higher mass ions of the substituted group $C_{11}H_8N^+$ (154) and $C_{12}H_{10}N^+$ (168)

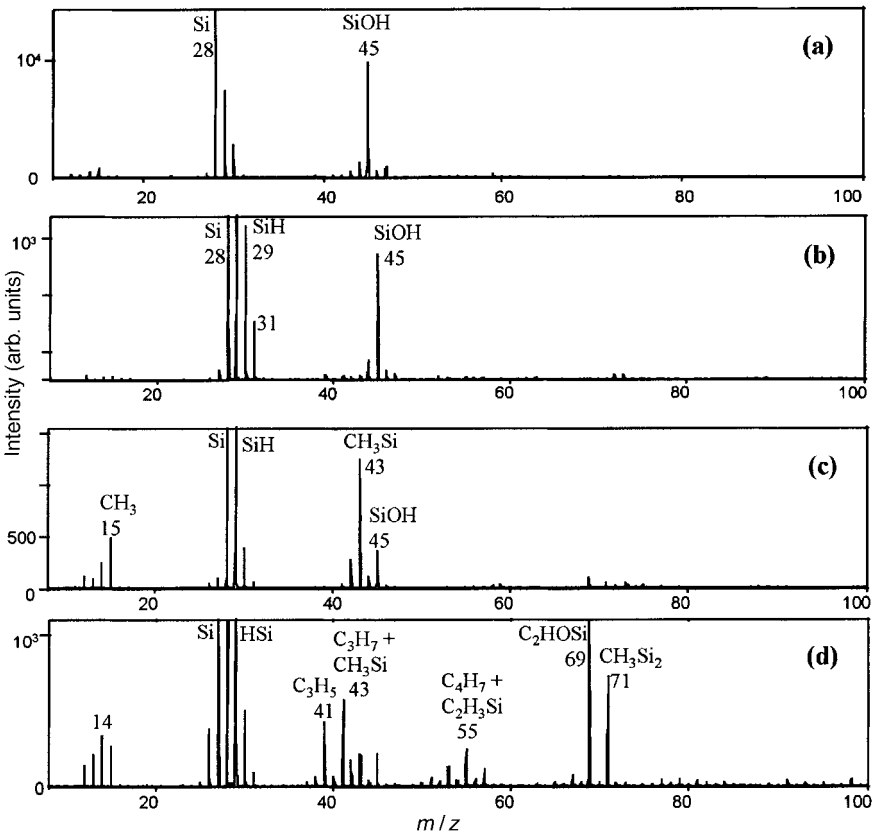

Fig. 2 Positive ion TOF-SIMS spectra of (a) SiO_2 **X17**, (b) $HSiO_{1.5}$ **X1**, (c) $CH_3SiO_{1.5}$ **X2**, (d) $CH_2{=}CHSiO_{1.5}$ **X4**

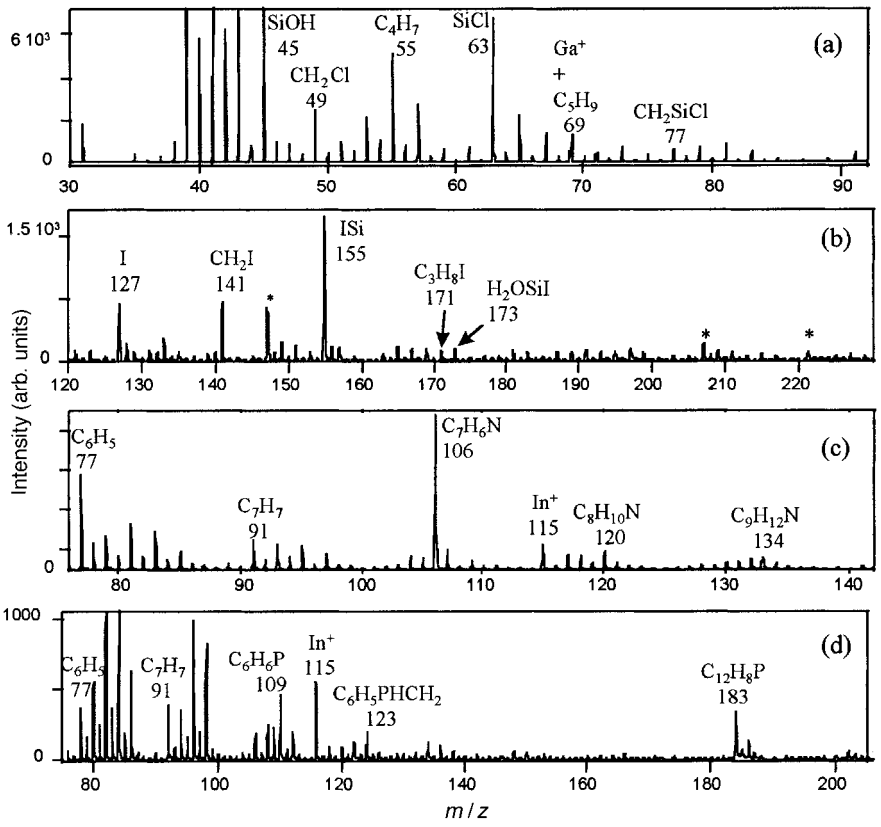

Fig. 3 Positive ion TOF-SIMS spectra of (a) $ClCH_2SiO_{1.5}$ **X3**, (b) $ICH_2CH_2CH_2SiO_{1.5}$ **X5**, (c) $C_6H_5NHCH_2CH_2CH_2SiO_{1.5}$ **X13**, (d) $(C_6H_5)_2PCH_2CH_2SiO_{1.5}$ **X14**

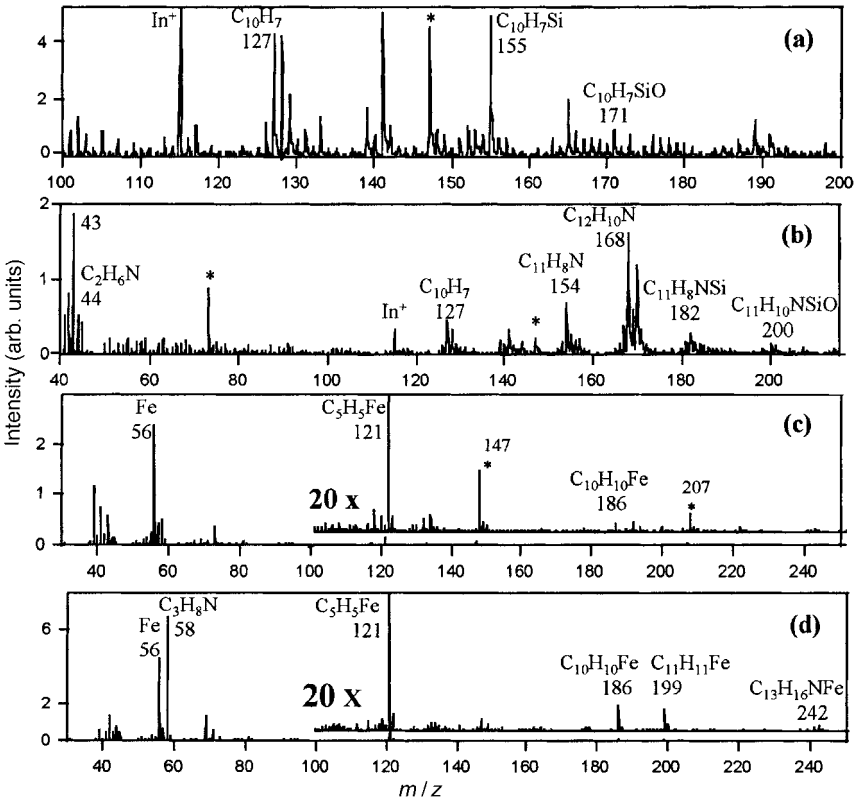

Fig. 4 Positive TOF-SIMS spectra of (a) $C_{10}H_7SiO_{1.5}$ **X10**, (b) $(CH_3)_2NC_{10}H_6SiO_{1.5}$ **X11**, (c) $C_5H_5FeC_5H_4SiO_{1.5}$ **X15**, (d) $C_5H_5FeC_5H_3N(CH_3)_2$-$SiO_{1.5}$ **X16**

are observed. For ferrocene gels **X15** and **X16**, peaks corresponding to the ferrocene group are the most prominent; peaks $^{56}Fe^+$, $C_5H_5^+$ (65), $C_5H_5Fe^+$ (121) for **X15** and peaks $^{56}Fe^+$, $C_3H_8N^+$ (58), $C_5H_5Fe^+$ (121), $C_5H_5FeCH_2^+$ (134), $C_{10}H_{10}Fe^+$ (186), $C_{11}H_{11}Fe^+$ (199), $C_{13}H_{16}FeN^+$ (242) for **X16** were clearly identified.

Besides evaluation of sample cleaning and control of the sol–gel process, TOF-SIMS investigations allow evaluation of the presence of characteristic ions from organic radicals in $RSiO_{1.5}$ xerogels. These observed ions cannot arise from precursor $RSi(OCH_3)_3$ species since other characteristic ions of precursors such as $SiOCH_3^+$ ($m/z=59$) are not present. The observed peaks correspond to the organic groups linked to silicon in such xerogels.

These peaks are sometimes weak in comparison to other hydrocarbon peaks, which may be due to their poor ionization yield but when easily ionizable functional groups are present in the organic moiety, characteristic ions from these groups are always present and readily identified. For the smallest organic groups bound to Si, ions corresponding to RSi or RSiO can also be observed. For the largest bulky organic groups, only fragment ions from the organic moiety can be observed.

The fact that characteristic ions from organic groups are present in the spectra cannot allow us to conclude about the hydrophilicity of the gels.

All the compounds reported here are hydrophobic, except for SiO_2 which is characterized by ions $^{28}Si^+$ and $SiOH^+$ (45) in a very clear mass spectrum. The relative intensity of the peak at $m/z=45$ should give an indication of the concentration of SiO bonds at the surface of samples; however not too much reliance should be given to this since the $SiOH^+$ peak is also intense for the $HSiO_{1.5}$ gel spectrum.

Ionization processes in TOF-SIMS analysis are not that clear and ionization yields of organic moieties of these xerogels are essentially unknown, therefore it is difficult to evaluate relative numbers of organic radicals *vs.* SiO bonds. Comparisons are only valid between similar compounds, for example between mono- and di-silylated gels with the same organic moiety.

Conclusion

The surface composition of monophasic hybrid organic–inorganic materials obtained by sol–gel hydrolysis–polycondensation of trialkoxysilanes $RSi(OR')_3$ has been analysed using time of flight-secondary ion mass spectrometry in positive and negative mode. All the results presented here show the presence of the organic moiety detected at the surface of the xerogels. When a halogen is present in the organic group, the negative ion spectra are of particular interest and clearly show the anion. Peaks corresponding to characteristic ions of the organic group R are always detected. In all cases, it is observed that organic group R is present at the surface of the solid. This result is in good agreement with earlier observations and shows that TOF-SIMS can be an efficient analytical tool to analyse the surface composition of MHOIM. For such nearly insoluble and amorphous solids, it seems to be the only way to locate the presence of the organic unit. The study of hybrid silica formed from polysilylated precursors is now in progress.

References

1 (*a*) H. K. Schmidt, *Mater. Res. Soc. Symp. Proc.*, 1984, **32**, 327; (*b*) H. K. Schmidt, *Inorganic and Organometallic Polymers, ACS Symp. Ser. no. 360*, American Chemical Society, Washington DC, 1988, p. 133; (*c*) H. K. Schmidt, *Mater. Res. Soc. Symp. Proc.*, 1990, **180**, 961 and references therein; (*d*) *Hybrid Organic–Inorganic Composites, ACS Symp. Ser. no. 585*, American Chemical Society, San Diego, 1994; (*e*) *New. J. Chem.*, 1994, **18**, 989; (*f*) P. Judenstein and C. Sanchez, *J. Mater. Chem.*, 1996, **6**, 511.

2 (*a*) G. Cerveau, C. Chorro, R. J. P. Corriu, C. Lepeytre, J. P. Lère-Porte, J. Moreau, P. Thépot and M. Wong Chi Man, *Hybrid Organic-Inorganic Silica Materials, ACS Symp. Ser. no. 585*, American Chemical Society, Washington DC, 1995, p. 210 and

references therein; (*b*) G. Cerveau, P. Chevalier, R. J. P. Corriu, C. Lepeytre, J. P. Lère-Porte, J. Moreau, P. Thépot and M. Wong Chi Man, *Tailor-made Silicon Oxygen Compounds. From Molecules to Materials*, ed R. Corriu and P. Jutzi, Vieweg Publ., 1996, p. 273 and references therein; (*c*) R. J. P. Corriu and D. Leclercq, *Angew. Chem. Int. Ed. Engl*., 1996, **35**, 1420 and references therein.
3 (*a*) P. Audebert, P. Calas, G. Cerveau, R. J. P. Corriu and N. Costa, *J. Electroanal. Chem*., 1994, **372**, 275; (*b*) P. Audebert, G. Cerveau, R. J. P. Corriu and N. Costa; *J. Electroanal. Chem*., 1996, **413**, 89.
4 G. Cerveau, R. J. P. Corriu and C. Lepeytre, *J. Mater. Chem*., 1995, **5**, 793.
5 G. Cerveau, R. J. P. Corriu and C. Lepeytre, *J. Organomet. Chem*., 1997, **548**, 99.
6 M. Pauthe, J. Phalippou, R. Corriu, D. Leclercq and A. Vioux, *J. Non-Cryst. Solids*, 1989, **113**, 21.
7 M. Pauthe, J. Phalippou, V. Belot, R. Corriu, D. Leclercq and A. Vioux. *J. Non-Cryst. Solids*, 1990, **125**, 187, 195.
8 S. J. Clarson, J. O. Stuart, C. E. Selby, A. Sabata, S. D. Smith and A. Ashraf, *Macromolecules*, 1995, **28**, 674.
9 F. Garbassi, E. Occhiello, C. Bastioli and G. Romano, *J. Colloid Interface Sci*., 1986, **117**, 258.
10 R. Dietrich, J. Grobe, B. Hagenhoff, K. Meyer and A. Benninghoven, in *Organosilicon Chemistry. From Molecules to Materials*, ed. N. Auner and J. Weis, VCH, Weinheim, 1994, p. 333.
11 J. Boyer, C. Brelière, F. Carré, R. J. P. Corriu, A. Kpoton, M. Poirier, G. Royo and C. Young, *J. Chem. Soc., Dalton Trans*., 1989, 43.
12 D. W. Slocum, B. W. Rockett and C. R. Hauser, *J. Am. Chem. Soc*., 1965, **87**, 1241.
13 V. Belot, R. J. P. Corriu, D. Leclercq, P. H. Mutin and A. Vioux, *J. Non-Cryst. Solids*., 1992, **147**–**148**, 309 and references therein.
14 U. Schubert, N. Hüsing and A. Lorenz, *Chem. Mater*., 1995, **7**, 2010 and references therein.
15 V. Belot, R. J. P. Corriu, D. Leclercq, P. H. Mutin and A. Vioux, *J. Non-Cryst. Solids* 1992, **147**–**148**, 52, and references therein.
16 G. Cerveau, R. J. P. Corriu and N. Costa, *J. Non-Cryst. Solids*., 1993, **163**, 226.
17 A. Delcorte, P. Bertrand, X. Arys, A. Jonas, E. Wischerhoff, B. Mayer and A. Laschewsky, *Surf. Sci*., 1996, **366**, 149.
18 R. J. P. Corriu, D. Leclercq, A. Vioux, M. Pauthe and J. Phalippou, in *Ultrastructure Processing of Advanced Ceramics*, ed. J.D. Mackenzie and D. R. Ulrich, Wiley, New York, 1988, p. 113.
19 M. Magi, E. Lippmaa, A. Samoson, G. Engelhart and A. R. Grimmer, *J. Phys. Chem*., 1984, **88**, 1518.
20 E. A. Williams, in *NMR Spectroscopy of Organosilicon Compounds in the Chemistry of Organosilicon Compounds*, ed. S. Patai and Z. Rappoport, Wiley, New York, 1989, p. 511.
21 M. G. Voronkov and V. J. Lavrent'yev, *Top. Curr. Chem*., 1982, **102**, 199 and references therein.
22 D. A. Loy, G. M. Jamison, B. M. Baugher, E. M. Russick, R. A. Assink, S. Prabakar and K. J. Shea, *J. Non-Cryst. Solids*, 1995, **186**, 44.
23 A. M. Fauk, W. H. Hines, K. E. Medzimradsky, M. A. Baldwin and B. W. Gibson, *J. Am. Mass. Spectrom*., 1993, **4**, 882.
24 D. A. McCrery, D. A. Peake and M. L. Gross, *Anal. Chem*., 1985, **57**, 1181.

Paper 8/02003E; *Received* 12*th March*, 1998